Superexchange-Mediated Ferromagnetic Coupling in Two-Dimensional Ni-TCNQ Networks on Metal Surfaces

N. Abdurakhmanova,[1] T.-C. Tseng,[1] A. Langner,[1] C. S. Kley,[1] V. Sessi,[2] S. Stepanow,[1] and K. Kern[1,3]

[1]*Max-Planck-Institut für Festkörperforschung, Heisenbergstrasse 1, D-70569 Stuttgart, Germany*

[2]*European Synchrotron Radiation Facility, BP 220, F-38043 Grenoble, France*

[3]*Institut de Physique de la Matière Condensée, Ecole Polytechnique Fédérale de Lausanne, CH-1015 Lausanne, Switzerland*

(Received 21 September 2012; published 11 January 2013)

We investigate the magnetic coupling of Ni centers embedded in two-dimensional metal-coordination networks self-assembled from 7,7,8,8-tetracyanoquinodimethane (TCNQ) molecules on Ag(100) and Au (111) surfaces. X-ray magnetic circular dichroism measurements show that single Ni adatom impurities assume a spin-quenched configuration on both surfaces, while Ni atoms coordinating to TCNQ ligands recover their magnetic moment and exhibit ferromagnetic coupling. The valence state and the ferromagnetic coupling strength of the Ni coordination centers depend crucially on the underlying substrate due to the different charge state of the TCNQ ligands on the two surfaces. The results suggest a superexchange coupling mechanism via the TCNQ ligands.

DOI: 10.1103/PhysRevLett.110.027202 PACS numbers: 75.70.Ak, 33.15.Kr, 75.30.Et, 78.70.Dm

Low-dimensional magnetic nanostructures show interesting phenomena with a high potential for their integration in magnetic recording, spintronic, and sensing devices [1–3]. Besides bulk materials, considerable effort is dedicated to the synthesis and investigation of single molecule magnets and also to their deposition on surfaces [4–9]. Particularly, the magnetic properties of molecules with spin centers were intensively investigated on various metals revealing the importance of hybridization and charge transfer at the molecule-metal interface [10–17].

Here, we follow a different strategy by assembling molecule-based magnets directly on surfaces by magnetically coupling several periodically arranged metal centers using organic ligands. Achieving this goal is similarly challenging since the adsorption on a metal surface can significantly modify the chemical and electronic state of both organic and inorganic components. Particularly, the magnetic moments of the metal centers can be considerably reduced or even quenched due to screening by surface electrons [18–22]. Also, the chemisorbed organic ligands can undergo appreciable electron transfer and associated bond order changes [23,24].

Previous work demonstrated that highly ordered two-dimensional metal-organic structures can be readily produced via self-assembly of metal atoms and organic ligands codeposited on metal surfaces [25]. The coordination networks are fabricated with a high control over composition and structure. The metal adatoms form rather strong and directional coordination bonds to the ligands, which effectively decouples the metal adatoms from the surface yielding a more atomic, localized electronic structure of the metal centers [26,27]. Recent experiments showed that Fe centers incorporated in an organic network possess high spin moments where the magnetic anisotropy can be controlled through the ligand environment [27]. However, the metal centers behave as independent paramagnetic units and the ligand mediated magnetic coupling was not achieved so far.

In this Letter, we show by means of scanning tunneling microscopy (STM) and x-ray absorption spectroscopy (XAS) that Ni atoms and 7,7,8,8-tetracyanoquinodimethane (TCNQ) molecules form ordered adlayers on Ag(100) and Au(111) surfaces and exhibit ferromagnetic behavior. In contrast, Ni adatom impurities are nonmagnetic on both surfaces. Our experiments show that the d-electron occupation in the networks depends on the substrate, being close to d^9 and d^8 on Ag(100) and Au(111), respectively. This difference is ascribed partially to the charge state of TCNQ on the surfaces and to the associated different electron transfer channels between ligands and Ni adatoms.

Polarization-dependent XAS experiments were performed at the beam line ID08 of the European Synchrotron Radiation Facility using total electron yield detection. Magnetic fields were applied collinear with the photon beam at sample temperatures between 8 and 300 K. Reference [28] provides details of the experimental setup. Data for the TCNQ/Ag(100) adlayer were acquired at the HE-SGM beam line at BESSY. A linear background was subtracted for clarity. The metal substrates were prepared by sputter-anneal cycles. TCNQ (98%, Aldrich) was sublimed ($T = 400$ K) from a quartz crucible onto the substrate at 300 K. The subsequent Ni deposition was followed by annealing to 350 and 400 K for Au(111) and Ag(100), respectively, to promote the network formation. On Ag (100), distinct Ni-TCNQ$_x$ adlayers with $x = 1$, 2, 4 can be prepared at appropriate Ni:TCNQ concentration ratios [29], whereas on Au(111) only $x = 1$ networks form. The sample preparation was verified by STM before

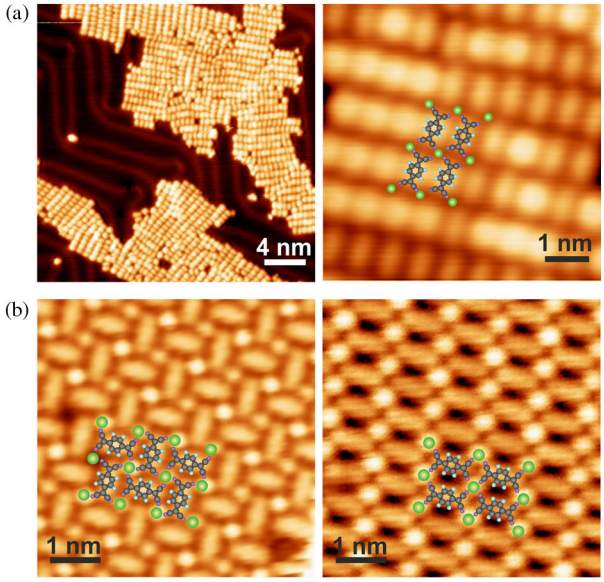

FIG. 1 (color online). STM topographs of Ni-TCNQ networks on (a) Au(111) and (b) Ag(100) surfaces. On Ag(100), two structures with the same stoichiometry coexist. The superposed models indicate the Ni (spheres) coordination arrangement. (Constant current STM: from top left to bottom right $I = 0.28$, 0.5, 0.26, 0.2 nA; sample bias $V = 1.3$, 1.2, -2, -1.3 V; $T = 5$ (a) and 300 K (b).

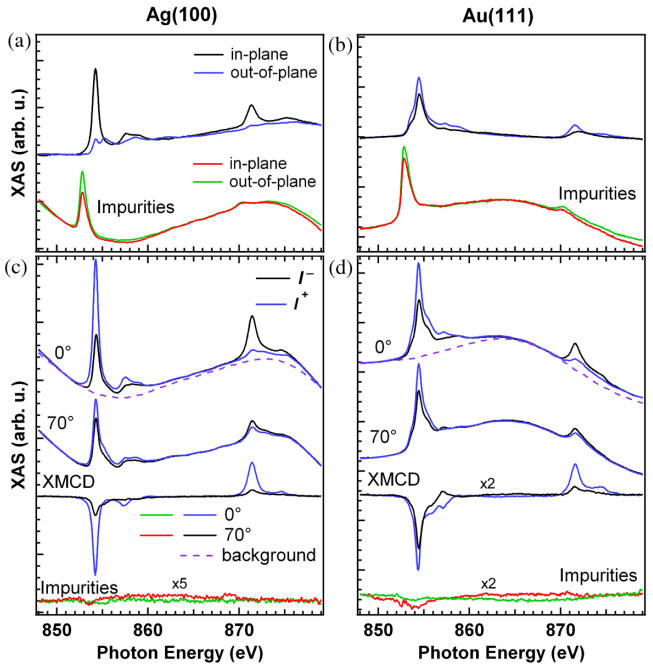

FIG. 2 (color online). XAS and XMCD of Ni-TCNQ and Ni impurities on (a),(c) Ag(100) and (b),(d) Au(111). Note that because of the low coverage the Ni XAS is superposed to the XAS background of the substrates. (a),(b) XAS with linear polarization parallel to the surface (in-plane) and at 20° to the surface normal (out-of-plane). ($B = 50$ mT; Ni-TCNQ $T = 300$ K, Ni impurities $T = 8$ K) (c),(d) XAS with circular polarization at 0° (normal) and 70° (grazing) incidence and the corresponding XMCD spectra. ($B = 5$ T, $T = 8$ K) The substrate background XAS is shown for normal incidence for a better identification of the Ni XAS features.

transferring the samples to the x-ray magnetic circular dichroism (XMCD) chamber without breaking the vacuum. Ni impurities were deposited onto clean surfaces directly in the XMCD chamber with the sample at 8 K to avoid clustering and alloying of Ni atoms.

Figure 1 shows STM topographs of Ni-TCNQ networks on Au(111) and Ag(100) with a stoichiometry of 1:1 that were investigated in this study. Each molecule forms four bonds to Ni atoms via its cyano groups (cf. models in Fig. 1). On Ag(100), two isomeric structures coexist, i.e., with alternating and parallel alignment of TCNQ molecules [Fig. 1(b) adapted from Ref. [29]], while on Au(111) only the parallel alignment was found. Moreover, the networks on Au(111) are inhomogeneous and grow only in small domain sizes (≈ 10 nm). The Ni centers form a lattice with a spacing of 7.2×11.3 Å^2 and 11.9×11.9 Å^2 in the domains of parallel and alternating TCNQ ligands, respectively.

Figures 2(a) and 2(b) show XAS spectra recorded at the Ni $L_{2,3}$ edge with linear polarization for impurities and networks on Ag(100) and Au(111). Note, that because of the low coverage the Ni XAS is superposed to a temperature dependent extended x-ray absorption fine structure background of the substrates. Background data are exemplarily shown in Figs. 2(c) and 2(d). The Ni coverage is estimated to 0.03 and 0.02 monolayers for the network and impurity samples, respectively. The latter is determined from the XAS L_3 intensity in comparison with the networks. The spectra of Ni impurities on both surfaces are nearly identical and show a single and narrow L_3 peak at 852.8 eV and an almost vanishing L_2 intensity. The small x-ray linear dichroism (XLD), i.e., the difference between spectra with out-of-plane and in-plane polarization of the E vector, signifies a larger fraction of empty states with out-of-plane lobes. The spectra differ clearly from bulk ferromagnetic Ni, where the ground state is proposed to be a mixture of d^8, d^9, and d^{10} configurations [30–32]. Here, the XAS resembles that of a d^9 system where the nearly vanishing L_2 edge suggests that only transitions from the initial $j = 5/2$ to the final $j' = 3/2$ states occur [33]. Further, a satellite feature present in bulk samples [30] that is ascribed to configurational mixing [31] is absent for the impurities.

The XAS data of the Ni-TCNQ networks exhibit pronounced differences. First, the spectra are shifted to higher photon energies by about 1.5 eV, which indicates the formation of strong chemical bonds to TCNQ resulting in charge depletion at the Ni atoms. The linearly polarized XAS for Ni-TCNQ/Ag(100) show a single L_3 peak and pronounced L_2 intensity with satellite features 3.5 and 4.5 eV above the main L_3 intensity. Further, the out-of-plane spectrum reveals a hump 1 eV above the reduced

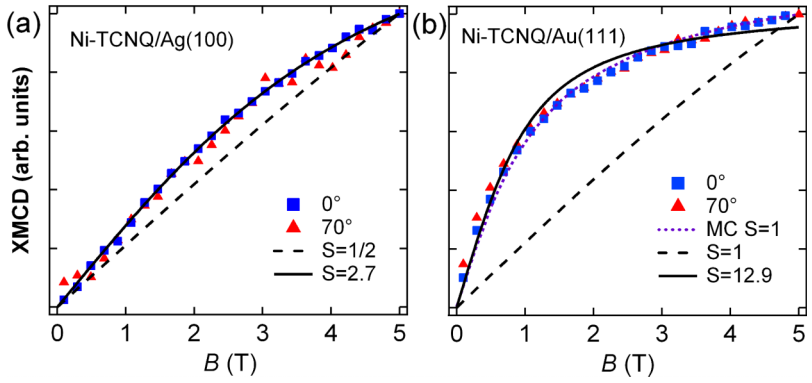

FIG. 3 (color online). Magnetization curves for Ni-TCNQ structures on (a) Ag(100) and (b) Au(111) obtained as the L_3 peak height vs magnetic field ($T = 8$ K).

L_3 onset. The strong XLD indicates an electronic ground state with a single in-plane hole, and thus a predominant d^9 character resembling that of Cu ions in the CuPc/Ag(100) system [28]. The satellite features are attributed to configurational mixing of d^8 and d^9 states due to bonding to the cyano groups of the ligands [31,34] and interaction with the surface electrons [10]. The Ni centers on Au(111) behave differently as evidenced by the weak XLD in Fig. 2(b) and a spectral shoulder at the low energy side of the L_3 peak. However, the satellite features 2.8 and 4.2 eV above the main peak resemble that on Ag(100). Compared to the XAS of the impurities also the L_2 edge shows small XLD having higher intensity for the out-of-plane polarization. The relatively small XLD demonstrates an isotropic distribution of holes in the d shell. Moreover, the presence of multiplet features further indicates that the Ni centers on Au(111) are closer to their atomic d^8 state.

The XAS spectra for parallel (I^+) and antiparallel (I^-) alignment of the photon helicity with the magnetic field B at normal (0°) and grazing (70°) x-ray incidence are presented in Figs. 2(c) and 2(d). The corresponding XMCD spectra, defined as $I^- - I^+$, are shown at the bottom of the panels. The nearly vanishing XMCD of the Ni impurities demonstrates that their magnetic moment is quenched on both surfaces, in line with previous reports [18,19], but in contradiction with a theoretical prediction [22]. Hence, we conclude that Ni adatoms hybridize strongly with the substrate and are spin-quenched due to strong correlation effects [35].

In contrast, the XMCD of coordinated Ni atoms shows sizeable magnetic moments. The anisotropic line shapes reflect the low coordination environment of the metal atoms similar to the XLD. On Ag(100), the apparent strong anisotropy of the XMCD is ascribed to the giant anisotropic contribution of the spin dipole moment $\langle T_z \rangle$ due to the d^9 character of the ground state [28,36]. Further, at 0° the XMCD spectra exhibit clear satellite features 3.1 and 3.9 eV above the L_3 and L_2 edge, respectively, and show a small shoulder 0.8 eV at 70° above the main L_3 peak. The XMCD spectra on Au(111) differ clearly from the Ag substrate. Here, the line shape shows pronounced differences between 0° and 70°, particularly at the satellite feature 2.7 eV above the L_3 peak. While the main XMCD features are similar on both surfaces, the anisotropy of the spectral intensity is smaller on Au(111) in line with the XAS analysis. These observations suggest that different bonding and electron transfer channels are present in the networks on the two substrates, as will be discussed below.

The magnetic interaction between the individual Ni centers is revealed in the magnetization curves obtained as the XMCD L_3 peak intensity ($T = 8$ K) normalized to 1 at $B = 5$ T for comparison (see Fig. 3). On both surfaces the magnetic susceptibility shows no apparent anisotropy. However, on Au(111) the curves show a stronger S shape compared to Ag(100). Already the weak S shape for the Ag sample suggests a small ferromagnetic coupling between the Ni centers. Fitting the curves with a Brillouin function yields a moment of $S_{\mathrm{fit}} = 2.7$ [assuming an isotropic $g = 2$ factor; this is justified by the small orbital moments obtained from the XMCD sum rule analysis (see below)]. This value suggests a large orbital moment, since we expect a $S = 1/2$ system for a d^9 shell, which is unlikely for a single-hole system in a low crystal field environment. For comparison, Fig. 3(a) shows also the magnetization curve of uncoupled $S = 1/2$ spins. The experimental data show clearly a higher susceptibility. The ferromagnetic coupling is even more evident on Au(111) [Fig. 3(b)], where the Brillouin function fit yields a large moment of $S_{\mathrm{fit}} = 12.9$. Note that the fit differs strongly above 1 T from the experimental data. The behavior of a paramagnetic $S = 1$ system (assuming a d^8 shell) is plotted as well. We interpret the considerably stronger susceptibility of the networks as ferromagnetic coupling between the Ni centers, since the large fitted S_{fit} moment cannot be attributed to a sizable orbital moment or magnetic anisotropy.

This interpretation is further corroborated by the analysis of the spin and orbital moments employing the XMCD sum rules (see Table I) [37,38]. In the analysis, the isotropic XAS is approximated by $3/2(I^+ + I^-)$ and obtained by subtraction of the substrate background XAS. The

TABLE I. Spin and orbital moments per hole determined from the XMCD sum rules. Estimated error is 20%.

	S_{eff}/hole		L_z/hole	
θ	Ag(100)	Au(111)	Ag(100)	Au(111)
0°	0.84	1.00	0.076	0.14
55°	...	0.58	...	0.14
70°	0.19	0.41	0.036	0.13

uncertainty in this procedure accounts for the relatively large error of 20% for the moments. While this is a good approximation for the rather isotropic spectra on Au(111), the XAS at grazing incidence for Ag(100) was multiplied by $2/(\cos^2 70° + 1)$ to account for the strong XLD [28]. Since the exact number of holes is not known, we report the effective moments per hole. Both systems show a strong apparent spin moment anisotropy. For the Ag(100) system we attribute this behavior to the strong anistropy of the T_z contribution to the effective spin moment $S_{z,\text{eff}} = S_z + 7/2T_z$ [28]. For the Au(111) sample the magnetization is close to saturation at 5 T; hence, the T_z term must also be strongly anisotropic. Both systems possess small but non-vanishing orbital moments. While on Ag(100) the orbital moment has an out-of-plane component twice as large as the in-plane component, there is nearly no anisotropy on Au(111). In both cases, the small magnitude of the orbital moment on Ag(100) [28] and the absence of orbital moment anisotropy on Au(111) are in agreement with the nearly isotropic magnetization curves [39].

Both networks on Ag(100) and Au(111) are similar in structure; i.e., single Ni atoms coordinate to four TCNQ ligands forming a quasirectangular superstructure. However, the valence state and the strength of the magnetic coupling of the Ni centers exhibits pronounced differences while the adatom impurities are very similar on the two substrates. We attribute this behavior partly to the charge state of the molecules on the different substrates as evidenced by the nitrogen K-edge XAS spectra shown in Fig. 4. TCNQ adsorbs weakly on Au(111) and remains in its neutral form [40]. The XAS spectra resemble that of TCNQ powder [23]; however, the strong angular anisotropy is due to the flat molecular adsorption geometry. In contrast, on Ag(100) TCNQ is negatively charged as evidenced by the disappearance of the first resonance at 397.4 eV in the nitrogen XAS. This behavior is very similar to TCNQ adsorbed on Cu(100) [23]. Upon coordination to Ni atoms the nitrogen XAS is nearly identical for the Ag (100) system, whereas on Au(111) electrons are donated from Ni to the molecules resulting in the redistribution of spectral intensity and charging of the molecules similar to the Ag(100) surface. Thus, we ascribe the different electronic configurations of the Ni centers in the networks partly to the distinct charge states of the free ligand on the two surfaces. Other important contributions to the magnetic coupling and electronic state of the Ni centers

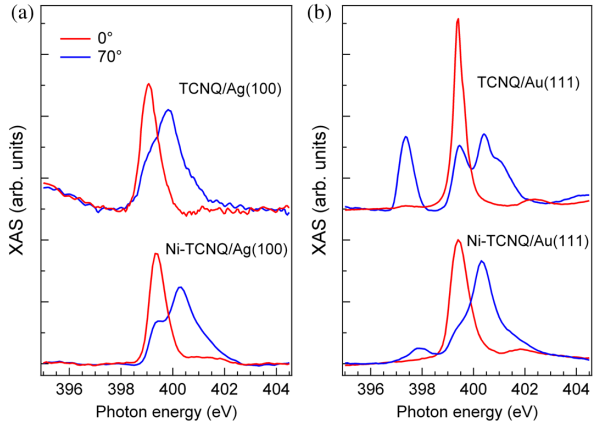

FIG. 4 (color online). Nitrogen K-edge XAS spectra with linear polarization parallel (0°) and nearly perpendicular (70°) to the surface for (a) Ag(100) and (b) Au(111) (300 K). Upper spectra: molecular phase, lower spectra: Ni-TCNQ.

on the two surfaces lie in the details of the coordination geometries as well as the orientation of the ligands on the surfaces.

To obtain further information on the magnetic coupling strength, we simulated the magnetization curves for Ni-TCNQ/Au(111) with a model spin Hamiltonian $H = -J\sum S_i S_j + gB\sum_i S_i$ with nearest neighbor interaction only using a Monte Carlo scheme for a two-dimensional grid of $S = 1$ spins ($g = 2$, $T = 8$ K). The result agreeing best with the data was obtained with $J = 0.27$ meV and is shown in Fig. 3(b) (MC $S = 1$). The magnitude of the exchange constant J indicates that a surface mediated RKKY interaction is unlikely [41,42]. We ascribe the ferromagnetic coupling to a superexchange mechanism via the TCNQ ligands as in the bulk compounds [43]. Further, the relative strength of the superexchange interaction on the two substrates is attributed to the different charge transfer channels in the Ni-TCNQ bonding. The stronger ferromagnetic coupling on Au(111) could be due to the direct bond formation and electron transfer between Ni adatoms and TCNQ ligands. Furthermore, the low hybridization of the molecules with the Au surface would hinder the screening of the ligand spin by surface electrons.

In summary, we have shown by means of XMCD that the magnetic moments of Ni adatom impurities on the surfaces of Au(111) and Ag(100) are quenched in agreement with earlier experimental observations [18]. Upon coordination to TCNQ the Ni atoms recover their magnetic moments and show ferromagnetic coupling. The electronic configuration and strength of the magnetic coupling depends crucially on the susbtrate, with stronger ferromagnetic interaction on the Au compared to the Ag surface. The results suggest a superexchange coupling mechanism via the negatively charged TCNQ ligands. The difference in the coupling strength and the electronic structure is traced back partly to the distinct charge state of TCNQ and charge transfer mechanisms between Ni and ligand molecules on

the two surfaces. The results demonstrate the direct synthesis of planar two-dimensional metal-organic magnets on metal surfaces that opens up a new route in the design, fabrication and investigation of low-dimensional magnetic materials at surfaces. The metal centers can be effectively decoupled from the metal surface by lateral coordination bonds and the magnetic coupling can be mediated and tuned through the organic ligands. Future experiments may address the tuning and enhancement of the magnetic coupling between the metal adatoms embedded in the organic matrix.

[1] L. Bogani and W. Wernsdorfer, Nat. Mater. **7**, 179 (2008).
[2] S. D. Bader, Rev. Mod. Phys. **78**, 1 (2006).
[3] C. Carbone *et al.*, Adv. Funct. Mater. **21**, 1212 (2011).
[4] J. S. Miller, Chem. Soc. Rev. **40**, 3266 (2011).
[5] A. Cornia, M. Mannini, P. Sainctavit, and R. Sessoli, Chem. Soc. Rev. **40**, 3076 (2011).
[6] M. Mannini *et al.*, Nature (London) **468**, 417 (2010).
[7] V. Corradini *et al.*, Phys. Rev. B **79**, 144419 (2009).
[8] S. Stepanow *et al.*, J. Am. Chem. Soc. **132**, 11 900 (2010).
[9] A. Lodi-Rizzini *et al.*, Phys. Rev. Lett. **107**, 177205 (2011).
[10] S. Stepanow, P. S. Miedema, A. Mugarza, G. Ceballos, P. Moras, J. C. Cezar, C. Carbone, F. M. F. de Groot, and P. Gambardella, Phys. Rev. B **83**, 220401(R) (2011).
[11] H. Wende *et al.*, Nat. Mater. **6**, 516 (2007).
[12] M. Bernien *et al.*, Phys. Rev. Lett. **102**, 047202 (2009).
[13] J. Miguel, C. F. Hermanns, M. Bernien, A. Krüger, and W. Kuch, J. Phys. Chem. Lett. **2**, 1455 (2011).
[14] C. Wäckerlin, D. Chylarecka, A. Kleibert, K. Müller, C. Iacovita, F. Nolting, T. A. Jung, and N. Ballav, Nat. Commun. **1**, 61 (2010).
[15] A. Scheybal, T. Ramsvik, R. Bertschinger, M. Putero, F. Nolting, and T. A. Jung, Chem. Phys. Lett. **411**, 214 (2005).
[16] F. Petraki, H. Peisert, F. Latteyer, U. Aygül, A. Vollmer, and T. Chassé, J. Phys. Chem. C **115**, 21334 (2011).
[17] T. Lukasczyk, K. Flechtner, L. R. Merte, N. Jux, F. Maier, J. M. Gottfried, and H.-P. Steinrück, J. Phys. Chem. C **111**, 3090 (2007).
[18] H. Beckmann and G. Bergmann, Phys. Rev. B **54**, 368 (1996).
[19] B. Lazarovits, L. Szunyogh, and P. Weinberger, Phys. Rev. B **65**, 104441 (2002).
[20] P. Lang, V. S. Stepanyuk, K. Wildberger, R. Zeller, and P. H. Dederichs, Solid State Commun. **92**, 755 (1994).
[21] R. Podloucky, R. Zeller, and P. H. Dederichs, Phys. Rev. B **22**, 5777 (1980).
[22] I. Cabria, B. Nonas, R. Zeller, and P. H. Dederichs, Phys. Rev. B **65**, 054414 (2002).
[23] T.-C. Tseng *et al.*, Nat. Chem. **2**, 374 (2010).
[24] Y. Zou, L. Kilian, A. Schöll, T. Schmidt, R. Fink, and E. Umbach, Surf. Sci. **600**, 1240 (2006).
[25] S. Stepanow, N. Lin, and J. V. Barth, J. Phys. Condens. Matter **20**, 184002 (2008).
[26] S. L. Tait, Y. Wang, G. Costantini, N. Lin, A. Baraldi, F. Esch, L. Petaccia, S. Lizzit, and K. Kern, J. Am. Chem. Soc. **130**, 2108 (2008).
[27] P. Gambardella *et al.*, Nat. Mater. **8**, 189 (2009).
[28] S. Stepanow, A. Mugarza, G. Ceballos, P. Moras, J. C. Cezar, C. Carbone, and P. Gambardella, Phys. Rev. B **82**, 014405 (2010).
[29] T.-C. Tseng, N. Abdurakhmanova, S. Stepanow, and K. Kern, J. Phys. Chem. C **115**, 10211 (2011).
[30] C. T. Chen, F. Sette, Y. Ma, and S. Modesti, Phys. Rev. B **42**, 7262 (1990).
[31] G. van der Laan and B. T. Thole, J. Phys. Condens. Matter **4**, 4181 (1992).
[32] T. Jo and G. A. Sawatzky, Phys. Rev. B **43**, 8771 (1991).
[33] G. van der Laan and B. T. Thole, Phys. Rev. B **42**, 6670 (1990).
[34] R. K. Hocking, E. C. Wasinger, F. M. F. de Groot, K. O. Hodgson, B. Hedman, and E. I. Solomon, J. Am. Chem. Soc. **128**, 10 442 (2006).
[35] A. C. Hewson, *The Kondo Problem to Heavy Fermions* (Cambridge University Press, Cambridge, England, 1993).
[36] J. Stöhr and H. König, Phys. Rev. Lett. **75**, 3748 (1995).
[37] B. T. Thole, P. Carra, F. Sette, and G. van der Laan, Phys. Rev. Lett. **68**, 1943 (1992).
[38] P. Carra, B. T. Thole, M. Altarelli, and X. Wang, Phys. Rev. Lett. **70**, 694 (1993).
[39] P. Bruno, Phys. Rev. B **39**, 865 (1989).
[40] I. F. Torrente, K. J. Franke, and J. I. Pascual, Int. J. Mass Spectrom. **277**, 269 (2008).
[41] E. Simon, B. Újfalussy, B. Lazarovits, A. Szilva, L. Szunyogh, and G. M. Stocks, Phys. Rev. B **83**, 224416 (2011).
[42] P. N. Patrone and T. L. Einstein, Phys. Rev. B **85**, 045429 (2012).
[43] G. Long and R. D. Willet, Inorg. Chim. Acta **313**, 1 (2001).